

Contemporary and relict processes in a coastal acid sulfate soil sequence: microscopic features

R.M. Poch¹, R.W. Fitzpatrick², B.P. Thomas², R.H. Merry², P.G. Self³ and M.D. Raven²

¹University of Lleida, Av. Rovira Roure 191, 25198 Lleida, Catalonia Spain. Email: rosa.poch@macs.udl.es

²CSIRO Land & Water/ University of Adelaide, Private Bag No. 2, Glen Osmond, S.A., 5064. Emails: brett.thomas@csiro.au; rob.fitzpatrick@csiro.au; richard.merry@csiro.au; mark.raven@csiro.au

³University of Adelaide, Email: peter.self@adelaide.edu.au

Abstract

In this study we use soil micromorphology and electron microscopy (SEM, TEM) to describe detailed morphological and compositional changes, together with mineral weathering pathways and mechanisms that occur at sub-microscopic scale in coastal acid sulfate soils, under varying environmental conditions in the Barker Inlet, South Australia. These approaches enabled correlation of micromorphological pedo-features and mineralogical results with pedo-geomorphic and soil data, to help construct 4D mechanistic models explaining soil-landscape processes at different time scales.

Optical microscopy of thin sections, SEM, TEM and X-ray diffraction were conducted on: a) two Histic-Sulfidic Intertidal Hydrosols (Protothionic Histosols; Terric Sulphihemist and Terric Sulphisaprist) in a tidal mangrove region at St Kilda and b) Sulfuric Hypersalic Hydrosols (Orthithionic Fluvisol; Hydraquentic Sulfaquepts) in the Gillman area, where tidal flushing was excluded in 1954 causing the formation of sulfuric horizons that overly sulfidic material. Pyrite framboids and cubes formed in sulfidic material associated with sapric and hemic materials. Oxidation products were iron oxyhydroxide pseudomorphs after pyrite. Gypsum crystallised after oxidation when a local source of calcium, such as shells or calcareous sand was provided, under water-saturated conditions. Jarosite hypocoatings formed along coarse biogenic voids during sporadic oxidation episodes.

These mineral transformations occurred over a very short range as a result of the high spatial variability of soil physico-chemical characteristics. This information was used to construct detailed mechanistic models to illustrate the interrelationships of pyrite, gypsum, jarosite and organic matter that can be used to help predict soil evolution under changing hydrological and environmental conditions.

Key Words

Mineralogy, micromorphology, organic materials, mechanistic model, soil classification.

Introduction

This paper is the second of two papers describing the pedo-geomorphic (Thomas *et al.* 2004) and micro-scale processes of sulfidic materials, sulfuric horizons and complex relict horizons in coastal acid sulfate soils (ASS) ranging from intertidal to supratidal areas and their drained equivalents in the Barker Inlet, South Australia. Integrated micromorphological/ electron microscopic research with pedo-geomorphic studies is a powerful tool to help understand complex processes in coastal ASS. However, the literature associated with micromorphological and pedo-geomorphic studies of coastal ASS is not extensive in Mediterranean environments, especially in Australia. Soil micromorphology can be defined as the *in situ* study of the structure of spatial patterns in natural and non-natural (disturbed) layers using microscopic techniques (Stoops 2003). In this study, we use soil micromorphology, scanning electron microscopy (SEM) and transmission electron microscopy (TEM) to describe and characterise the imprints of physical, chemical and biological processes (changes in) on coastal ASS. More specifically, we have used these techniques to define the source of the mineral (e.g. pyrite, gypsum and jarosite) and organic matter fractions (i.e. sapric and hemic materials) together with weathering pathways and mechanisms that occur at sub-microscopic scale under changing hydrological and environmental conditions. This has been the only thin section, micromorphological study of sulfidic materials and sulfuric horizons in coastal ASS in southern Australia. This work compliments that of Bush and co-workers (Bush and Sullivan 1999) on ASS of the north coast of NSW.

Setting and general characteristics

The two coastal ASS sequences studied are located in Barker Inlet, near Adelaide, South Australia (Figure 1).

They consist of:

- Natural tidal mangrove soils with sulfidic material occurring at St Kilda, which classify as Histic-Sulfidic Intertidal Hydrosols (Isbell 1996). Profile 600 is 0.5 m thick and located 500 m from the low tide mark at the seaward fringe of the mangrove forest. Profile 2610 is 2m thick and is located 50 m from the low tide mark at the seaward fringe of the mangrove forest (Figure 1).
- Drained tidal mangrove soils with sulfuric horizons overlying sulfidic material occurring at Gillman, which classify as Sulfuric Hypersalic Hydrosols (Isbell 1996). Profile BG11 originally developed in a supratidal regime but tidal inundation was totally excluded in 1954 when a bund wall was constructed causing oxidation of sulfidic material. The parent material occurs in several layers of lacustrine and tidal sediments deposited under mangrove and samphire vegetation (Figure 1).

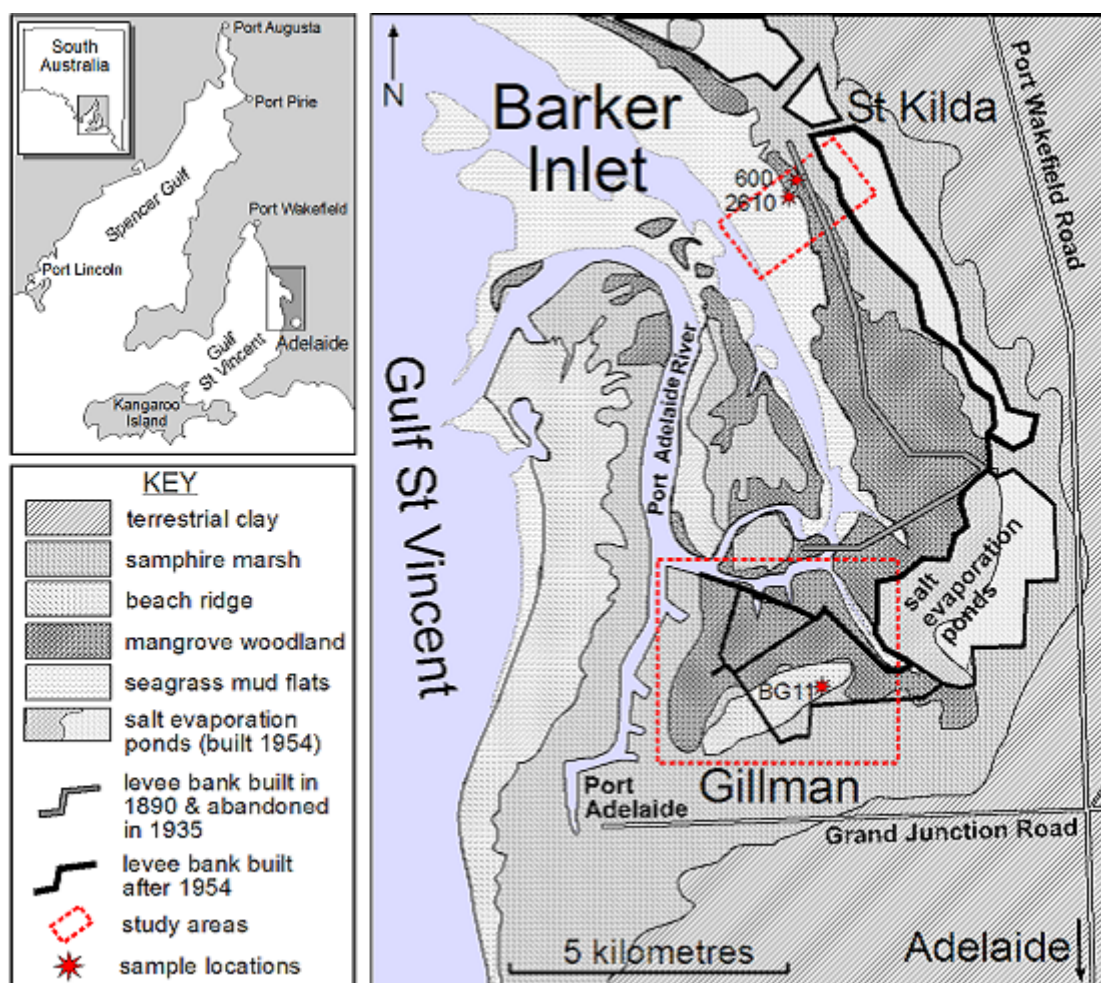


Figure 1. Barker Inlet is a tidal dominated estuary located 20kms north of Adelaide, South Australia. Soil profiles 600 and 2610 are located at St Kilda in a “natural” mangrove woodland. Soil profile BG11 is located at Gillman. It was drained in the mid 1950s when a bund wall was constructed in an attempt to reclaim inter-tidal mangrove woodlands and samphire salt marsh for agriculture and industry. The land was soon abandoned due to severe acidification, salinity and storm-water ponding.

Methods

Horizontal and vertical thin sections were made from undisturbed soil blocks of surface and subsurface horizons of profiles 600, 2610 and BG11 (Salins and Ringrose-Voase 1994). The study and description of the thin sections followed the guidelines and terminology of Stoops (2003). SEM and EDAX studies were made on polished blocks and thin sections, and TEM studies (not reported here) were made on clay fractions. Powder X-ray diffraction (XRD) investigations used to confirm mineralogy were made on finely ground samples using a Philips PW1800 microprocessor-controlled diffractometer using Co K-alpha radiation.

Results and discussion

Organic matter characteristics and pyrite formation in mangrove soils (Histic-Sulfidic Intertidal Hydrosols) at St Kilda

Soil classification

These saturated, intertidal soils have horizons that include sulfidic material (qualify as sulfidic) because they have a natural pH of 7.5, and, when incubated as a layer 1 cm thick under moist conditions, while maintaining contact with the air at room temperature, show a marked drop in pH to a value of 4 or less within 8 weeks (Soil Survey Staff 2003). A feature of these soils is that they contain horizons with different kinds of organic soil materials - as defined by the amount of rubbed fibre content (sapric has <17% by volume rubbed fibre, hemic > 40% rubbed fibre and fibric >75% rubbed fibre) (Soil Survey Staff 2003). Hence horizons that contain predominantly sapric material have a high degree of decomposed plant materials from which the organic materials are derived. This is used to determine the kind of organic materials when classifying soils (Soil Survey Staff 2003; Isbell 1996).

Profile 600 consists of a hemic Oa horizon overlying a sapric C horizon and classifies as a Terric Sulfihemist (Soil Survey Staff 2003) and Protothionic Histosol (FAO 1998). Profile 2610 consists of a thin layer of hemic material at the near surface (Oa1) with thick underlying layers of sapric material (Oa2, Oa3 and C) and classifies as a Terric Sulfisaprist (Soil Survey Staff 2003) and Protothionic Histosol (FAO 1998). Both these Histic-Sulfidic Intertidal Hydrosols (Isbell 1996) overly unconsolidated Holocene coastal marine sediments consisting of saturated, light grey, shelly and often silty or clayey sands (St Kilda formation). Some morphological, chemical and mineralogical characteristics are given by Fitzpatrick *et al.* (1996), Fitzpatrick and Self (1997) and Thomas *et al.* (2004).

Surface layers with predominantly hemic material

The surface horizons (Oa) of profiles 600 and 2610 have high porosities (80%) because they contain a high proportion of fibres. These layers are classified as hemic material because they contain moderately decomposed organic materials. In thin section many of the recognizable organic residues are anisotropic due to the preservation of cellulose and form the rubbed fibre.

These surface horizons contain primarily a mixture of yellowish, amorphous organic matter (highly decomposed organic matter) and recognizable organic tissues and plant organs (less decomposed fibre). The latter are altered to different degrees due to physical breakdown by fauna and chemical alteration consisting of blackening and formation of phlobaphene, a brown tannin oxidation product very resistant to decomposition (Bullock *et al.* 1985). Profile 2610 has more reddish, phlobaphene-rich organic residues than 600 (Figure 2).

Subsurface layers with predominantly sapric material

The sapric materials contain less organic tissue (i.e. fibres) and more yellow, gelatinous, amorphous organic matter (Figure 2). Lee and Mannock (1974) also described a brown amorphous matrix in drained sapric material, with a strong aggregation in pellets due to faunal activity. The sapric material has a lower porosity consisting of vesicles and vughs. Therefore its permeability is lower than the hemic material, which has more conducting porosities due to packing pores between fibres. The amorphous organic material is polymorphic (De Coninck *et al.* 1974), mixed with clay and has a granular structure due to faunal activity. The amorphous material has a layered structure alternating with horizontal tissue and organ residues in the deeper horizons. In some areas cracks have formed, possibly due to desiccation. The amorphous material has a yellowish colour with opaque, highly reflecting spots, which occur inside yellowish aggregates distant from the pore walls. The coarse material consists of fine muscovite flakes, diatoms and quartz grains.

Some blackened fibres appear to have transformed to opaque intercalations because they are often found around tissue residues. These intercalations consist of amorphous black materials. Less frequently the black material forms hypocoatings in the yellow organic groundmass. Microprobe analysis of the yellow organic groundmass indicates a higher clay content than the black organic materials. Implications are that the yellow organic materials are older and more stable. A common characteristic is the high Na, Cl and S

contents, which indicates the capacity of the amorphous organic matter to scavenge and retain these elements from seawater.

Pyrite formation

Pyrite cubes and framboids (maximum diameter of 10 μm) embedded and dispersed in organic matter were observed in SEM images of profile 600. Sulfide composition of the framboids is mainly pyrite (Fe_2S) with a few having monosulfide (FeS_{2-x}) composition. This is unexpected given the S/Fe ratio of the organic matter, mostly higher than 2, which should promote the formation of monosulfides. This suggests that Fe is the limiting factor for the formation of pyrite. A grain of chalcopyrite was identified in a blackened tissue residue. Some inclusions of detrital CaCO_3 and halite crystals have been observed in tissue residues.

Pyrite framboids are larger (up to 50 μm) and well formed in profile 2610 (Figure 2). They occur as nests up to 200 μm wide, but are also frequently occur as singular and dispersed framboids in the organic groundmass. The framboids consist of pyrite cubes with sizes from 0.5 to 2 μm , with different degrees of packing (Figure 2). Fine gypsum crystals occur in the groundmass and as nests of very fine prismatic crystals up to 2 μm in length within tissue residue (Figure 2). The morphology of the prismatic gypsum crystals indicates they are formed *in situ* at very low pH values (Cody and Cody 1988). Only tissue channels could provide sufficient aeration during low tides to cause oxidation of the pyrite or sulfide ions retained in the organic matter to lower the pH and promote gypsum precipitation. The source of calcium could be from detrital calcareous material or shell fragments. Pyrite oxidation is more limited in the sapric groundmass because the porosity of the amorphous organic material is low, consisting of non-conducting pores as vughs and vesicles.

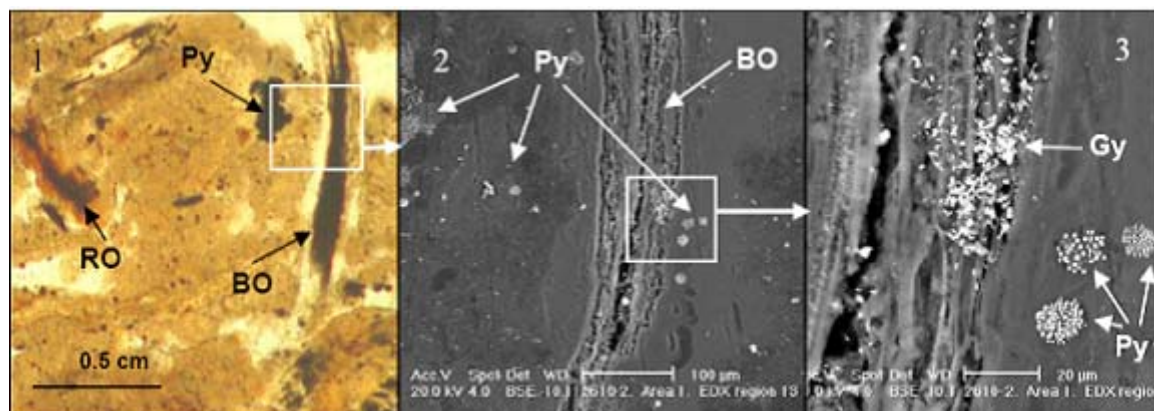


Figure 2. Sapric material in Profile 2610, with blackened and red phlobaphene-rich tissue residues included in a groundmass of yellow, amorphous polymorphic organic matter; pyrite framboids and gypsum crystals in one of the residues. BO: black organic matter, RO: red organic matter, Py: pyrite, Gy: gypsum. Image 1: Plane polarised light (PPL). Images 2 (350 μm across) and 3 (80 μm across) are Backscatter Secondary Electron Images (BSEI).

Micromorphologically, profile 2610 shows a better formation of pyrite, a higher degree of decomposition of organic matter (less blackened residues) and a lower conductive porosity than 600. These characteristics are in agreement with more anoxic conditions that exist in profile 2610 (Thomas *et al.* 2004). In contrast, Rabenhorst and Lindbo (1998) reported that more black organic matter forms in soils with “more wetness” but in soils undergoing podsolization (more aeration) more light (brown) organic matter forms.

Pedogenic processes in drained coastal soil (BG11)

Soil classification and morphological description

Soil profile BG 11 is a 1.95 m thick epipedon, and consists of horizons with five clear lithological discontinuities. A “sulfuric horizon” is defined as being composed of either mineral or organic soil material (15 cm or more thick) that has both $\text{pH} < 3.5$ and bright yellow jarosite mottles. The soil has a sulfuric horizon and classifies as a Hydraquentic Sulfaquept (Soil Survey Staff 2003), Orthithionic Fluvisol (FAO 1998) and Sulfuric Hypersalic Hydrosol (Isbell 1996). The properties of profile BG11 reflect the presence of the lithological discontinuities and the processes that have acted on them:

waterlogging and desiccation of the swamp. The present macro and micromorphology are summarized in Figure 3 below.

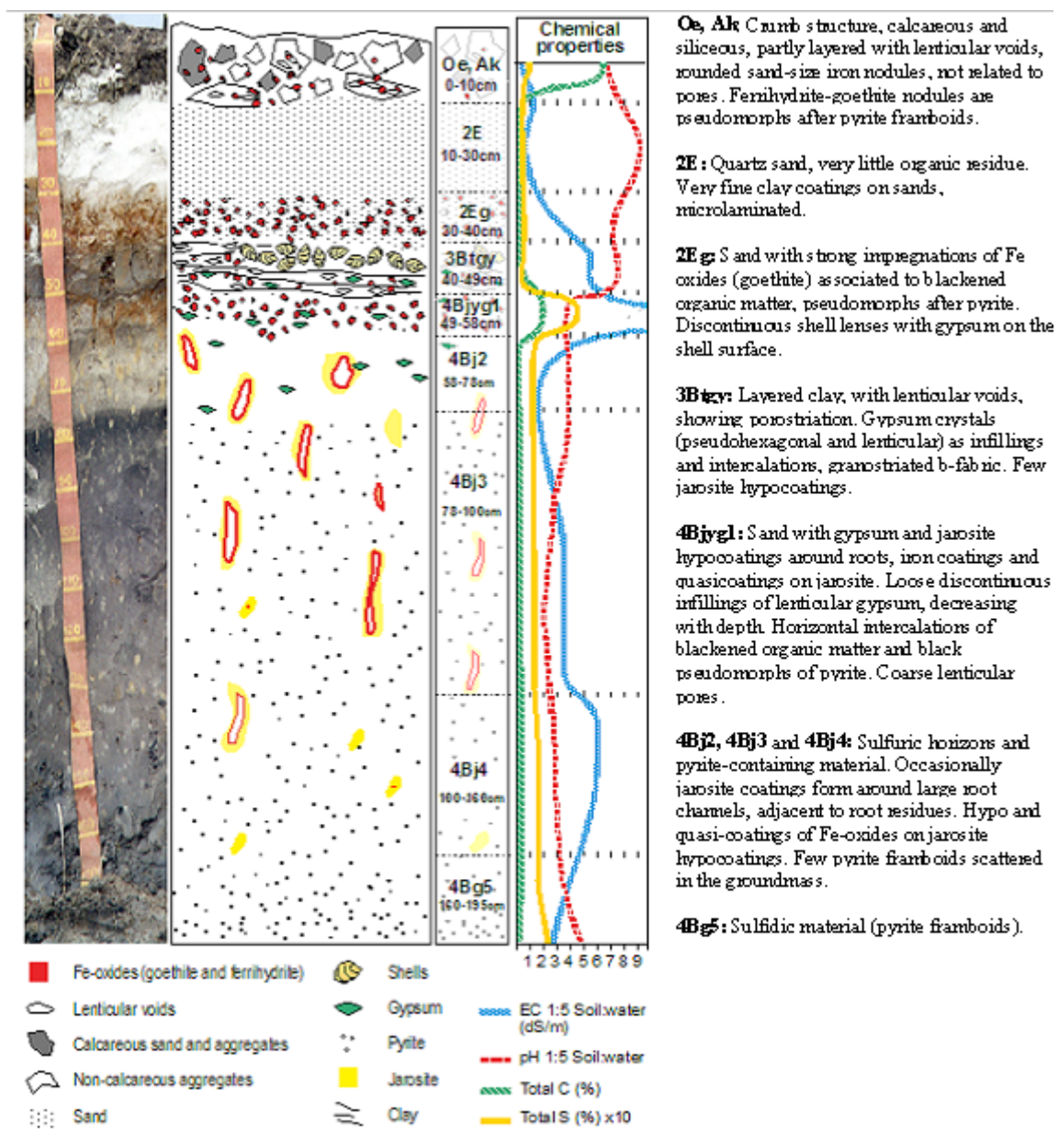


Figure 3. Main macro and micromorphological features of actual Acid Sulfate Soil profile BG11.

The **surface horizons (Oa and A)** have a well developed crumb structure, formed by a mixture of calcareous and non-calcareous aggregates that are partly layered, with horizontal planar and lozenge-shaped (lenticular) voids, showing granostriation. The lenticular voids can be attributed to gypsum lenses formed in water-saturated conditions and dissolved after the soil was drained. The A Horizon also shows nodules of Fe-oxides in the aggregates, not related to pores, after pyrite framboids formed under past anaerobic conditions. Following drainage, their rapid oxidation in a calcareous environment produced an *in situ* precipitation of Fe-oxides, a process also observed by Miedema *et al.* (1974). The whole structure is at present altered by biological activity. Jarosite is absent because of the presence of CaCO_3 .

The underlying **E horizons** consist of sands, lacking organic matter except near the lower boundary (**horizon 2Eg**), where there are frequent iron coatings and hypocoatings near plant remains. Iron nodules are pseudomorphs of pyrite framboids which have originated from fast pyrite oxidation in a calcareous environment, similar to the overlying Oa horizon.

The **3Btgy horizon** has a similar structure as the lower Oa horizon: layered clays alternating with organic intercalations, lenticular voids and porostriation. The boundary with the overlying sands is abrupt and precludes any illuvial origin of the clays. Between these two horizons there are discontinuous lenses of decalcifying shells. The most remarkable pedo-features are the ones related to iron, frequent gypsum lenses in the clay matrix and jarosite coatings. The horizontal structure of the clays and the abundance of well preserved organic matter is due to sedimentation under moist conditions that favoured pyrite formation. When the water table lowered, Fe-oxide pseudomorphs formed as pyrite was oxidised. Due to the lower permeability of the clays, a perched watertable developed on top of the layer. As pH became acidic due to sulfide oxidation, shells began to dissolve and Ca was released allowing gypsum formation. Gypsum crystal growth occurs on shell surfaces. Little jarosite is present in this horizon, in places with less calcium availability as the shell layer is discontinuous and irregular. Since the water table is enriched with calcium, it is able to moisten the clay layer during dry periods (no bypass flow) and gypsum precipitates within the clays. This is evident by the poro- and granostriation textures observed, indicating displacive crystallization. No gypsum infillings were observed, which would form by capillary rise of gypsum-saturated water. Pseudo-hexagonal and lenticular gypsum are found together, which indicates different formation conditions. Organic matter and pH are two of the factors controlling the morphology: lenses would form in neutral to basic pH in presence of organic matter (Cody and Cody 1998). Due to the relatively high solubility of gypsum, several cycles of dissolution-precipitation have occurred since primary gypsum formed. Changes in the formation conditions, mostly Ca saturation and pH of the soil solution, have probably taken place, resulting in different gypsum crystal morphologies (shapes). Many of the original gypsum crystals have been dissolved, shown by the abundance of lenticular pores with porostriation. The lenticular habit of the primary gypsum crystals indicates they formed at near neutral pH, due to a calcareous environment.

Horizon 4Bjyg1 shows the same features as the previous horizon, but in a much sandier matrix. Gypsum is generally lenticular, but also rombohedral and pseudo-hexagonal. It occurs as intercalations and infillings. Jarosite formation is general around pores, as coatings or hypocoatings. Fe-impregnating features occur as quasicocoatings or discontinuous coatings on the jarosite ones. Jarosite is more abundant, because as water percolates and gypsum precipitates, the soil solution is depleted of calcium and bicarbonate, loses its buffering effect and in some spots jarosite forms. It coexists with gypsum since the latter may have been formed at the beginning of the oxidation, when availability of calcium was higher. The appearance of the jarosite-impregnated groundmass with gypsum inclusions does not differ from the jarosite-free zones. This suggests that the jarosite hypo-coatings were probably formed after gypsum precipitated. Rapid oxidation of pyrite produces jarosite precipitations around it (Van Dam and Pons 1973). According to these authors, if oxidation is slow, sulfate and potassium migrate to pore walls and jarosite is formed as infillings, coatings or hypo-coatings of very fine crystals in pores. Fe coatings (not quasi-coatings) are explained by further hydrolysis of jarosite under a marked climatic seasonal difference. In our case the morphology of Fe coatings indicates they originated directly from pyrite oxidation in organic residues, which are adjacent to pores (Figure 4).

The underlying **4Bj2, 4Bj3 and 4Bj4 horizons** have undergone the same processes, but on a still sandier matrix than horizon 4Bj1. Gypsum is not well identified due to the similar birefringence as quartz, but there is less gypsum because of the depletion of Ca in the soil solution as it percolates down the profile. Jarosite becomes the main product of pyrite weathering along coarse pores, which are the first to aerate during oxidation, but it is also scattered in the groundmass, as fine pseudo-cubes 0.5 μm in size. This morphology of primary jarosite does not necessarily mean a pseudomorph transformation from pyrite, since they have the same crystal habit. EDAX analyses show that these jarosite cubes contain more K than the matrix, and also that there is an excess of S, which means that some pyrite is still present. Fe oxides are not as much related to the organic residues, pointing to a slower oxidation that allows the movement of Fe^{2+} further away from the original pyrite crystal site.

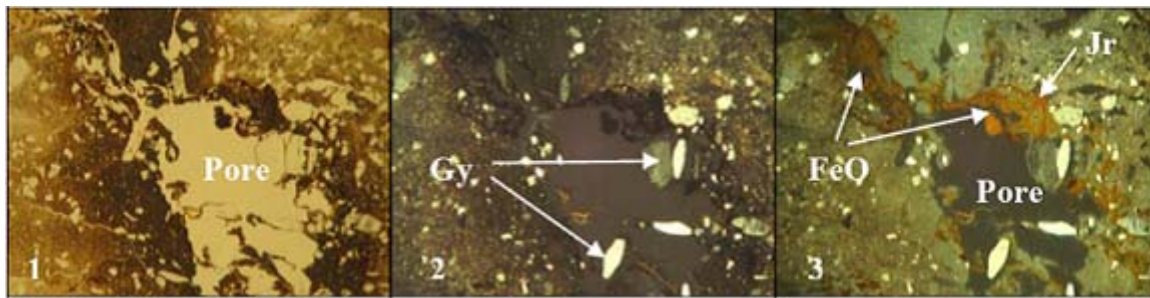


Figure 4. Thin section analysis of BG11, horizon 4Bjyg1 shows a pore with loose discontinuous gypsum in filling and lenticular gypsum crystals (Gy), orange Fe coating (FeO) and yellow jarosite (Jr) hypocointing. Field of view is 6.5 mm across. Image 1 is PPL, image 2 is XPL and image 3 is reflected light.

Horizon 4Bg5 contains abundant sulfidic materials; pyrite is present as scattered framboids in the groundmass or as aggregate nodules or clusters. There is oxidation only along large pores and jarosite is formed (Figure 5). The pH is not buffered as happens in the upper horizons due to calcite depletion. Amorphous silica could also be present (Van Dam and Pons 1973), derived from the weathering of clays, which become unstable at low pH. In our case very thin silica coatings could be present, but there is not much availability of weatherable clay in these two horizons to provide silica. NaCl salts have precipitated on quartz grains as needle-like crystals.

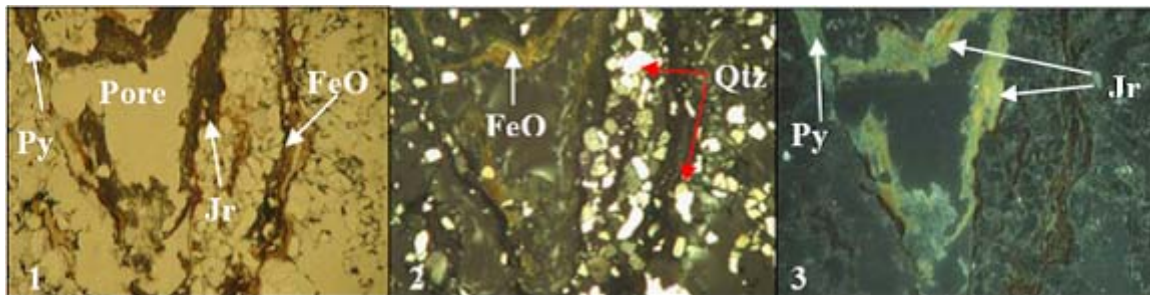


Figure 5. Thin section analysis of BG11, horizon 4Bg5 showing jarosite coating, Fe-hypo and quasicointings (FeO), yellow jarosite (Jr) hypocointing and pyrite quasicointing (Py) around a root channel with organic residues in a quartz (qtz) sand. There is no gypsum in this sample. Field of view is 4.2 mm across. Image 1 is PPL, image 2 is XPL and image 3 is reflected light.

Conclusion

Sapric material was more decomposed, less porous, more reduced and allowed the formation of larger pyrite crystals than hemic material. In the Histosols, limited oxidation of pyrite along coarse pores forms gypsum because of the presence of calcium (shells) in the environment. In the upper horizons of the drained coastal soil the rapid oxidation of pyrite in organic residues caused precipitation of iron oxides and lenticular gypsum, which was leached out of the profile afterwards (Figure 3). Jarosite becomes the main product of pyrite oxidation in the 4Bj horizons, due to decreasing availability of calcium. Some small pyrite framboids occur in the underlying sandy sulfuric horizons (4Bj3, 4Bj4). Coatings of jarosite and iron oxides form along large root channels during short periods of aeration. Micromorphological features identified in all soil layers, together with chemical, mineralogical and physical properties, help explain contemporary and relict processes in the development of these complex coastal acid sulfate soils. Microscopic features also verify soil characteristics that are used to classify these soils (Soil Survey Staff 2003; FAO 1998).

References

- Bullock P, Fedoroff N, Jongerijs A, Stoops G, Tursina T, Babel U (1985) 'Handbook for soil thin section description'. Waine Research Publications: Wolwerhampton, UK.
- Bush RT and Sullivan LA (1999) Pyrite micromorphology in three Australian Holocene sediments. *Australian Journal of Soil Research* **37**, 637-654.
- Cody RD, Cody AM (1988) Gypsum nucleation and crystal morphology in analog saline terrestrial environments. *Journal of Sedimentary Petrology* **58**, 247-255.

- De Coninck F, Righi D, Maucorps J, Robin AM (1974) Origin and micromorphological nomenclature of organic matter in sandy spodosols. In 'Soil Microscopy'. Ed GK Rutherford pp 263-273, 279-280 The Limestone Press: London
- FAO (1998) 'The world reference base for soil resources (WRB)' World Soil Resources Report No. 84. Food and Agriculture Organisation for the United Nations FAO/ISSS/AISS/IBG/ISRIC: Rome
- Fitzpatrick RW, Fritsch E, Self PG (1996) Interpretation of soil features produced by ancient and modern processes in degraded landscapes: V Development of saline sulfidic features in non-tidal seepage areas. *Geoderma* **69**, 1-29.
- Fitzpatrick RW, Self PG (1997) Iron Oxyhydroxides, Sulfides and Oxyhydroxysulfates as Indicators of Acid Sulfate Weathering Environments. *Advances in GeoEcology* **30**, 227-240.
- Isbell RF (1996) 'The Australian soil classification'. CSIRO Publishing: Melbourne
- Lee GB, Manock B (1974) Macromorphology and micromorphology of a Wisconsin Saprist. In 'Histosols – Their characteristics, classification and use'. Eds AR Aandahl, SW Buol, DE Hill, HH Bailey HH) pp 47-62. SSSA Special Publication Series 6 SSSA: Madison, Wisconsin
- Miedema R, Jongmans AG, Slager S (1974) Micromorphological observations on pyrite and its oxidations products in foru Holocene alluvial soils in the Netherlands. In 'Soil Microscopy. Proc. 4th Int. Working Meeting on Soil Micromorphology'. Ed GK Rutherford pp 772-794 The Limestone Press: London
- Rabenhorst MC, Lindbo DL (1998) Micromorphology of sandy epipedons along an upland-wetland transect. In 'Quantifying soil hydromorphology'. Eds MC Rabenhorst, JC Bell, PA McDaniel pp 195-208. SSSA Special Publication 54 SSSA: Madison, Wisconsin
- Salins I and Ringrose-Voase AJ (1994) Impregnation techniques for soils and clay materials - the problems and overcoming them. CSIRO (Australia) Division of Soils Technical Report 6/1994.
- Soil Survey Staff (2003) 'Keys to Soil Taxonomy. 9th edition'. (United States Department of Agriculture, Soil Conservation Service: Blacksburg) http://soils.usda.gov/technical/classification/tax_keys/
- Stoops G (2003) 'Guidelines for analysis and description of soil and regolith thin sections' Soil Science Soc Am: Madison, Wisconsin
- Thomas B, Fitzpatrick RW, Merry RH, Poch RM, Hicks WS and Raven MD (2004) Contemporary and relict processes in a coastal acid sulfate soil sequence: macroscopic and geomorphic features. Australian and New Zealand Third Joint Soils Conference: Oral Papers. 5-9 December 2004, The University of Sydney (this volume).
- Van Dam D, Pons LJ (1973) Micropedological observations on pyrite and its pedological reaction products. In 'Acid Sulphate Soils. Proc. Int. Symp. Acid Sulphate Soils, 13-20 Aug 72' Ed H Dost pp 169-195 Wageningen.